Song, X.H.; Liang, B.; Liu, G.F.; Li, R.; Xie, J.P.; Du, K.; Huang, D.Y.: Expression of a novel alternatively spliced variant of NADP(H)-dependent retinol dehydrogenase/reductase w...

ARTICLE *in* INTERNATIONAL JOURNAL OF CANCER · APRIL 2007

Impact Factor: 5.09 · DOI: 10.1002/ijc.22306 · Source: PubMed

Int. J. Cancer: **120,** 1618–1626 (2007)

Expression of a novel alternatively spliced variant of NADP(H)-dependent retinol dehydrogenase/reductase with deletion of exon 3 in cervical squamous carcinoma

Xu-Hong Song, Bin Liang, Ge-Fei Liu, Rui Li, Jian-Ping Xie, Kun Du and Dong-Yang Huang*

Center for Molecular Biology, Shantou University Medical College, Shantou, Guangdong 515041, People's Republic of China

NADP(H)-dependent retinol dehydrogenase/reductase (NRDR) plays an important role in maintaining the homeostasis of retinoid. Aberrations in retinoid metabolism are considered as early events in carcinogenesis. We identified a novel alternatively spliced variant, $NRDRB_1$, in HeLa cell and human cervical squamous carcinoma tissues, which is characterized by a complete deletion of exon 3. The latter resulted in changes in subcellular localization of $NRDRB_1$ when compared with the peroxisomal localization of NRDR. To clarify the clinical significance of $NRDRB_1$, we investigated its mRNA and protein expressions in normal cervical and cervical squamous carcinoma tissues, using RT-PCR, quantitative real-time PCR, Gateway expressing system, immunoprecipitation, immunoblotting, MALDI-TOF mass spectrometry and immunohistochemistry. We detected $NRDRB_1$ mRNA in 14 of 26 (53.9%) cervical cancer tissues, but in none of the 12 normal cervical tissues. $NRDRB_1$ protein was expressed in $NRDRB_1$ mRNA-positive cases. While the full-length NRDR mRNA was observed in both normal and neoplastic cervical tissues, its protein was only expressed in normal cervical epithelium. The results presented here provide evidence that metabolic disturbances of retinal and retinoic acid, due to abnormal splicing and functional disorder of NRDR, may be involved in cervical tumorigenesis.

Key words: NRDR; alternative splicing; tumorigenesis; cervical squamous carcinoma

The *NRDR* (*DHRS4*) gene is localized on 14q11.2 chromosome (Genbank accession number AB045131), and was initially purified from rabbit liver.[1] The gene is a member of the short chain alcohol dehydrogenase/reductase (SDR) superfamily and shares the basic structural and functional features of SDR.[2,3] In addition to its main activity as retinol dehydrogenase, NADP(H)-dependent retinol dehydrogenase/reductase (NRDR) displays high aldehyde reductase activity in retinoic acid (RA) metabolism.[1] Furthermore, recombinant mouse NRDR and human NRDR, which are localized to peroxisomes, exhibit NADP(H)-dependent retinol dehydrogenase/reductase activity.[4,5]

The pathway for RA synthesis consists of 2 sequential reactions.[6] Retinol is first oxidized to retinal, which is a reversible and rate-limiting step. Cytosolic alcohol dehydrogenase (ADH) and/or microsomal SDR are responsible for this reaction.[7] Retinal is then irreversibly and rapidly converted to RA by cytosol aldehyde dehydrogenase (ALDH)[8] and/or retinal oxidase.[9]

Reduction of retinal and generation of RA represents a controlled process for minimizing the steady-state concentrations of the intermediate product retinal, because of the potential toxicity of retinal and RA, and the time and locus requirements for RA. NRDR is distributed in many human organs and tissues,[5] because of its higher activity of retinal reductase at physiological pH than other enzymes of SDR[1,5]; it plays an important role in maintaining the homeostasis of retinal and RA.

A recent study demonstrated that functional disorders of the SDR or ADH family members increase the toxic levels of retinol, albeit levels far from levels expected to be encountered normally.[10] In experimental animals, retinol deficiency is associated with a higher incidence of cancer and increased susceptibility to chemical carcinogens. Clinical and experimental research also indicates the presence of abnormal metabolism of retinoids in some tumors and that such abnormality correlates with tumorigenesis.[11–19] We reported previously the presence of different alternative splicing variants of NRDR in human carcinoma cell lines,[20] further suggesting the close relationship between NRDR variants and tumorigenesis. Alternative splicing is also reported to be associated with various diseases.[21,22] Alternative splicing is a process in which identical pre-mRNA molecules are spliced in different ways, and this is important for creating protein diversity in the development of complex organisms.[23–27] Alterations in splicing have also been detected in various human cancers, and the vast majority of these changes are considered to be involved in tumorigenesis.[28–32]

To our knowledge, there is no information on the expression of NRDR variants in normal human cells and tumor tissues necessary to define the relationship between alternative splicing of NRDR and tumorigenesis. In the present study, we isolated and cloned a new variant of NRDR in HeLa cells. Using reverse transcription-polymerase chain reaction (RT-PCR), quantitative real-time PCR, Gateway expressing system, immunoprecipitation (IP), immunoblotting, matrix-assisted laser desorption/ionization time-of-flight (MALDI-TOF) mass spectrometry and immunohistochemistry, we examined normal human cervical epithelium and cervical squamous carcinoma for the expression of NRDR variants, to understand the role of these variants in the development of cervical cancer.

Material and methods

Cell culture and tumor-tissue samples

HeLa cells were cultured in RPMI 1640 supplemented with 10% fetal bovine serum (HyClone) at 37°C and 5% CO_2.

Histopathologically confirmed cervical squamous carcinoma tissues were obtained from patients with cervical tumors, and normal cervical tissues were obtained from patients who underwent hysterectomy for gynecopathalogical conditions at Shantou University Affiliated Hospital. The study protocol was approved by the Human Ethics Review Committee of Shantou University, and a signed consent form was obtained from each subject. The tissue samples were immediately frozen in liquid nitrogen and stored in a freezer at −80°C, until analysis.

RNA extraction, RT-PCR, 3′ and 5′ RACE assay

Total RNA was extracted from HeLa cell line and various tissue specimens, using the RNeasy Mini Kit (Qiagen, Hilden, Germany). RNA (1 μg) from each sample was reverse-transcribed into cDNA using a 2-strand cDNA synthesis kit (Promega, Madison, WI). The

Abbreviations: ADH, alcohol dehydrogenase; ALDH, aldehyde dehydrogenase; HPV, human papilloma virus; IP, immunoprecipitation; NRDR, NADP (H)-dependent retinol dehydrogenase/reductase; RA, retinoic acid; SDR, short chain alcohol dehydrogenase/reductase.

The first and second authors have contributed equally to this work and should be considered co-first authors.

Grant sponsor: National Natural Science Foundation of China; Grant number: 30470396.

***Correspondence to:** Center for Molecular Biology, Shantou University Medical College, 22 Xinling Road, Shantou, Guangdong 515041, People's Republic of China. Fax: +0086-754-8557562.
E-mail: huangdy@stu.edu.cn

Received 5 February 2006; Accepted after revision 7 August 2006
DOI 10.1002/ijc.22306
Published online 17 January 2007 in Wiley InterScience (www.interscience.wiley.com).

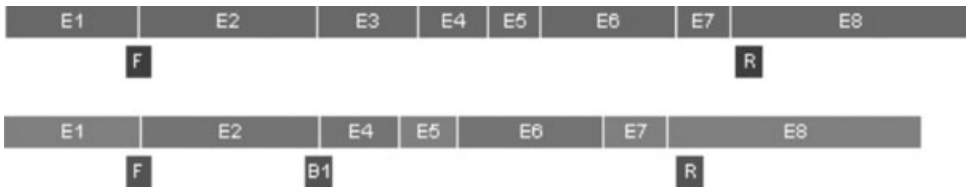

FIGURE 1 – Schematic illustration of primers for detection of NRDR and $NRDRB_1$. E1–E8 indicate 8 exons of NRDR, F: forward primer, NRDRF; R: reverse primer, NRDRR; B1: forward primer, NRDRB1F.

cDNAs (2 μl) from the cell line or tissues were amplified by PCR, using a forward primer NRDRF: 5′-TCC ACC GAC GGG ATC GGC TT-3′, and a reverse primer NRDRR: 5′-ATG CCA GCA CAA TCC TCT GGC T-3′. Figure 1 shows the primers used to amplify NRDR and $NRDRB_1$. $NRDRB_1$ expression was also detected using specific primers (the forward primer NRDRB1F: 5′-TGG TGG CCA CGA CTC TGG ACA TT-3′) spanning the region from exons 2 and 4 to exon 8 of the *DHRS4* gene (Fig. 1, NRDRB1F/NRDRR). The reaction parameters were 94°C for 45 sec, 58°C for 40 sec and 72°C for 1 min for 35 cycles, followed by 8-min extension at 72°C using Taq DNA polymerase (Medical & Biological Laboratories, Nagoya, Japan). To amplify full-length cDNA of $NRDRB_1$, the 3′RACE and 5′RACE were carried out using the protocol supplied by the manufacturer (Invitrogen, San Diego, CA), with slight modification using nested PCR.

The PCR products were analyzed by electrophoresis in 1.2% agarose gel, and the corresponding PCR products were gel-purified and cloned into pGEM-T Easy Vector System (Promega). Positive clones were sequenced by the dideoxynucleotide method (3100 DNA sequencer, Applied Biotech).

Quantitative real-time PCR analysis

Two set of primers used in this study were QB_1F: 5′-CTG GTG GCC ACG ACT CTG GAC ATT A-3′ and QB_1R: 5′-ACT GAG CCG CCT CCT CGT TTC-3′, QF: 5′-TAG TCT CCA ATG CTG CTG TCA-3′ and QR: 5′-AGC CGC CTC CTC GTT TCT-3′. The primers set was selected to amplify a 95-bp fragment of $NRDRB_1$ and 150-bp fragment of NRDR, respectively.

Total RNA was reversed using QuantiTect Reverse Transcription kit (Qiagen). The real-time PCR amplification reaction mixture (25 μl) contains 2 μl of cDNA sample, 0.75 μl of each primer (10 μM), 12.5 μl of QuantiTect SYBR Green PCR Master Mix (Qiagen) and 0.5 unit of uracil-*N*-glycosylase. The thermal cycling conditions comprised a carryover contamination prevention step at 50°C for 2 min, 95°C for 15 min to activate the HotStarTaq DNA Polymerase, 40 cycles at 94°C for 15 sec, 60°C for 30 sec and 72°C for 30 sec. Consequently, at the end of the PCR cycles, the real-time PCR products were immediately analyzed using a ramping rate of 0.03°C/sec from 60 to 95°C, to calculate the dissociation curve, to confirm that single PCR product was detected by SYBR Green I dye. No-template control reactions for every primer pair were also included on each reaction plate to check for external DNA contamination. Sequence-specific standard curves were generated using 10-fold serial dilutions of plasmid (pGEM-T easy vector; Promega) encompassing NRDR or $NRDRB_1$ cDNA. Real-time PCR reactions were performed, recorded and analyzed by using the ABI-Prism 7700 (Applied Biosystems, Foster City, CA). Each measurement of the sample was conducted in duplicate.

Expression of $NRDRB_1$ in Escherichia coli *and production of polyclonal antibody*

Bacterial expression plasmids were prepared by recombining the $NRDRB_1$ cDNA into pDEST14 vectors (Gateway Expression system, Invitrogen) to express the native protein without His-tag sequences. The constructs were transformed into *E. coli* BL21-AI cells (Invitrogen), and the open reading frame of the cDNA in the expression plasmid was verified by nucleotide sequence analysis.

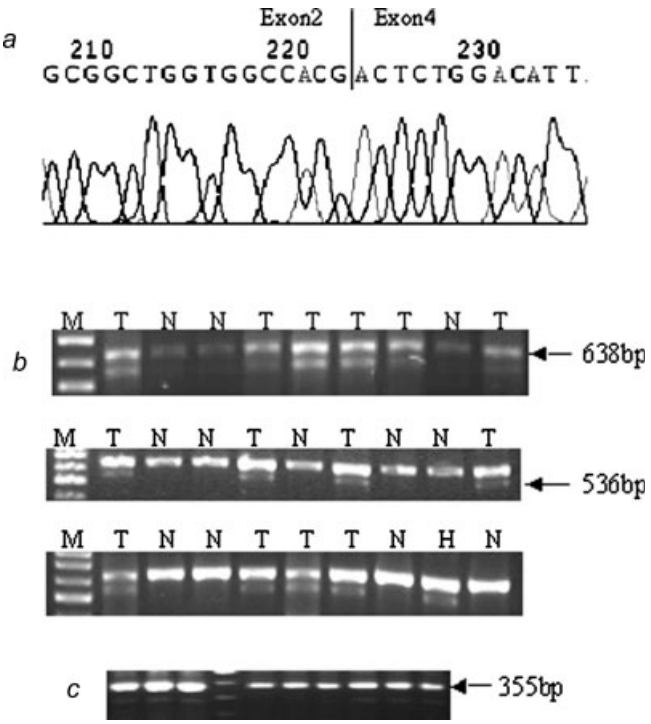

FIGURE 2 – Analyses of $NRDRB_1$ mRNA splice variant. (*a*) Sequencing result of $NRDRB_1$. (*b*) Expression of NRDR B_1 (536 bp) and NRDR (638 bp) in cervix tumor. $NRDRB_1$ transcripts were detected in 14 of 26. M: Molecular weight markers. N: normal cervix epithelium samples. T: cervix squamous carcinoma tissues. H: HeLa cell. (*c*) Representative analyses of $NRDRB_1$ mRNA splice variant in cervical tumor, using specific primer sequences for $NRDRB_1$ ($NRDRB_1$ F/NRDR R, Fig. 1).

Overexpression of a recombinant was induced at mid-log growth phase of BL21-AI (OD_{600} = 0.6) using 0.2% L-arabinose at 37°C. After the addition of L-arabinose, the cultures were continuously grown for 3 hr. The expressed $NRDRB_1$ native protein was purified using affinity chromatography, as described previously.[1] Polyclonal antibody of $NRDRB_1$ was produced using the purified native protein, as described previously.[33]

Anti-rabbit serum was isolated using the protein G column on ATKAexplore system (Amersham Biosciences, Arlington Heights, IL) using standard procedures. The sensitivity and specificity of the purified antibody were determined using dot blot and Western blot.

Transfection and immunofluorescence

For localization of $NRDRB_1$ in mammalian cells, another expression plasmid was constructed. The constructed vector pDEST53 (Invitrogen) for production of $NRDRB_1$ amino-terminal green fluorescence protein (GFP)-tagged protein was transfected into HeLa cells using Lipofectamine® (Invitrogen). As a positive control, the pDEST53 vector for production of amino-terminal

```
NRDR-P        MHKAGLLGLCARAWNSVRMASSGMTRRDPLANKVALVTASTDGIGFAI
NRDRB1-P      MHKAGLLGLCARAWNSVRMASSGMTRRDPLANKVALVTASTDGIGFAI

NRDR-P        ARRLAQDGAHVVVSSRKQQNVDQAVATLQGEGLSVTGTVCHVGKAEDR
NRDRB1-P      ARRLAQDGAHVVVSSRKQQNVDQAVATLQGEGLSVTGTVCHVGKAEDR

NRDR-P        ERLVATAVKLHGGIDILVSNAAVNPFFGSIMDVTEEVWDKTLDINVKAPAL
NRDRB1-P      ERLVAT                                TLDINVKAPAL

NRDR-P        MTKAVVPEMEKRGGGSVVIVSSIAAFSPSPGFSPVNVSKTALLGLTKTLAI
NRDRB1-P      MTKAVVPEMEKRGGGSVVIVSSIAAFSPSPGFSPVNVSKTALLGLTKTLAI

NRDR-P        ELAPRNIRVNCLAPGLIKTSFSRMLWMDKEKEESMKETLRIRRLGEPEDC
NRDRB1-P      ELAPRNIRVNCLAPGLIKTSFSRMLWMDKEKEESMKETLRIRRLGEPEDC

NRDR-P        AGIVSFLCSEDASYITGETVVVGGGTPSRL
NRDRB1-P      AGIVSFLCSEDASYITGETVVVGGGTPSRL
```

FIGURE 3 – Deduced amino acid sequence of NRDR and $NRDRB_1$. Boldface denotes cofactor binding, catalytic, and peroxisome targeting residues. The box indicates the "LVSNAA" fold.

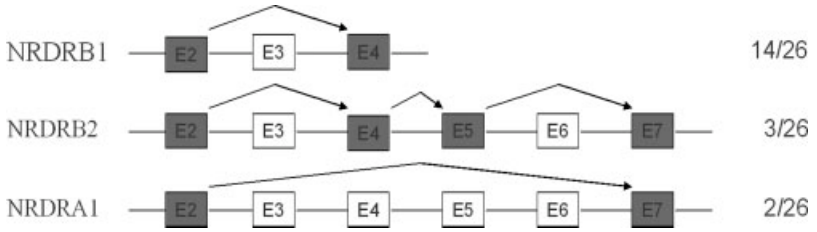

FIGURE 4 – Schematic illustration of 3 splicing variants of the *NRDR* gene. Arrows show the alternative splicing pattern. Shaded boxes show the region that was spliced into the mRNAs, and open boxes show the exon that was spliced out. The frequency of each splicing variant detected in tumor samples is shown at right. The open read frames of those variants are not destroyed. E, exon.

GFP-tagged NRDR fusion protein was transfected into HeLa cells and grown on coverslips. After 24-hr transfection, the cells were fixed in 4% paraformaldehyde in phosphate-buffered saline (PBS: 150 mM NaCl, 9.9 mM $Na_2HPO_4{\cdot}2H_2O$ and 1.6 mM KH_2PO_4) for 5 min and permeabilized in 0.2% Triton X-100, 0.04% SDS in PBS for 5 min. After blocking in PBS containing 3% bovine serum albumin (BSA) for 30 min, the primary monoclonal antibody for catalase (1:200 dilution, Sigma, St. Louis, MO) was incubated for 1 hr at room temperature. Secondary antibody IgG-cy3 (Chemicon International, Temecula, CA) was applied at a dilution of 1:400. Before mounting the coverslips, 300 nM 6-diamidino-2-phenylindole (DAPI, Sigma) in PBS was used for 5 min for nuclear staining. Finally, immunofluorescence staining was observed using an Olympus fluorescence microscope equipped with image acquisition system. Images were merged using Simple PCI (Compix, USA.).

IP and MALDI-TOF mass spectrometry assay

The HeLa cells and different samples were lysed or homogenized (Pierce, Rockford, IL) using a protease inhibitor cocktail (Sigma). Magnetic beads (Dynal Biotech, Oslo, Norway) were washed and coated with purified $NRDRB_1$ polyclonal antibody, 8 μg/10^7 beads. The lysate was clarified by centrifugation and the supernatant dissolved 1:2 in co-IP buffer (0.1 M Na-phosphate buffer, pH 7.4). The equivalent of 400 μg total protein was incubated with coated beads at 4°C for 24 hr under constant rotation. As a control, the same amount of lysate protein was incubated in the absence of the antibody. The complexes were subjected to 3 washes with co-IP buffer. The proteins were eluted with 0.1 M glycine (pH 2.7). The eluates were neutralized immediately and subjected to 12% sodium dodecyl sulfate–polyacrylamide gel electrophoresis (SDS-PAGE), and the immunoblot was analyzed. The positive bands stained with Coomassie Brilliant Blue were cut for peptide mass fingerprint (PMF) assay, using MALDI-TOF mass spectrometry (Shanghai Gene Core BioTechnologies, China).

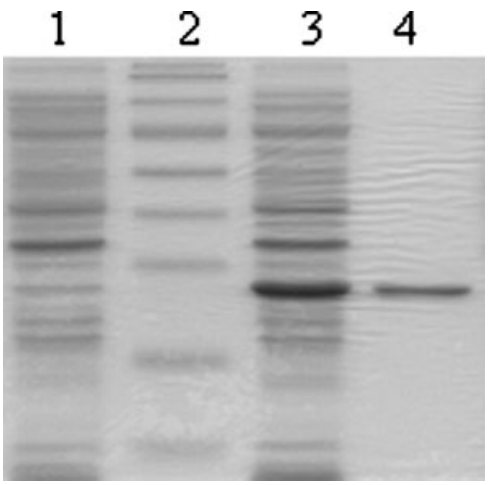

FIGURE 5 – Expression and purification of $NRDRB_1$ native protein. Samples of $NRDRB_1$-containing fractions were analyzed by SDS-PAGE and stained by Coomassie R-250. Lane 1, BL-21AI; Lane 2, molecular weight markers; Lane 3, cell lysate from BL-21AI transformed with the pDEST 14 vectors containing the $NRDRB_1$ gene; and Lane 4, purified soluble $NRDRB_1$.

Immunoblotting analysis

Samples eluted from IP were resolved using 12% SDS-PAGE and transferred to a nitrocellulose membrane (Hybond P, Amersham Life Science, Buckinghamshire, UK). The primary antibody was rabbit anti-$NRDRB_1$ polyclonal antibody, and the secondary antibody was goat anti-rabbit IgG conjugated to horseradish peroxidase (1:3,000, Pierce). Immunoblots were visualized on photo-

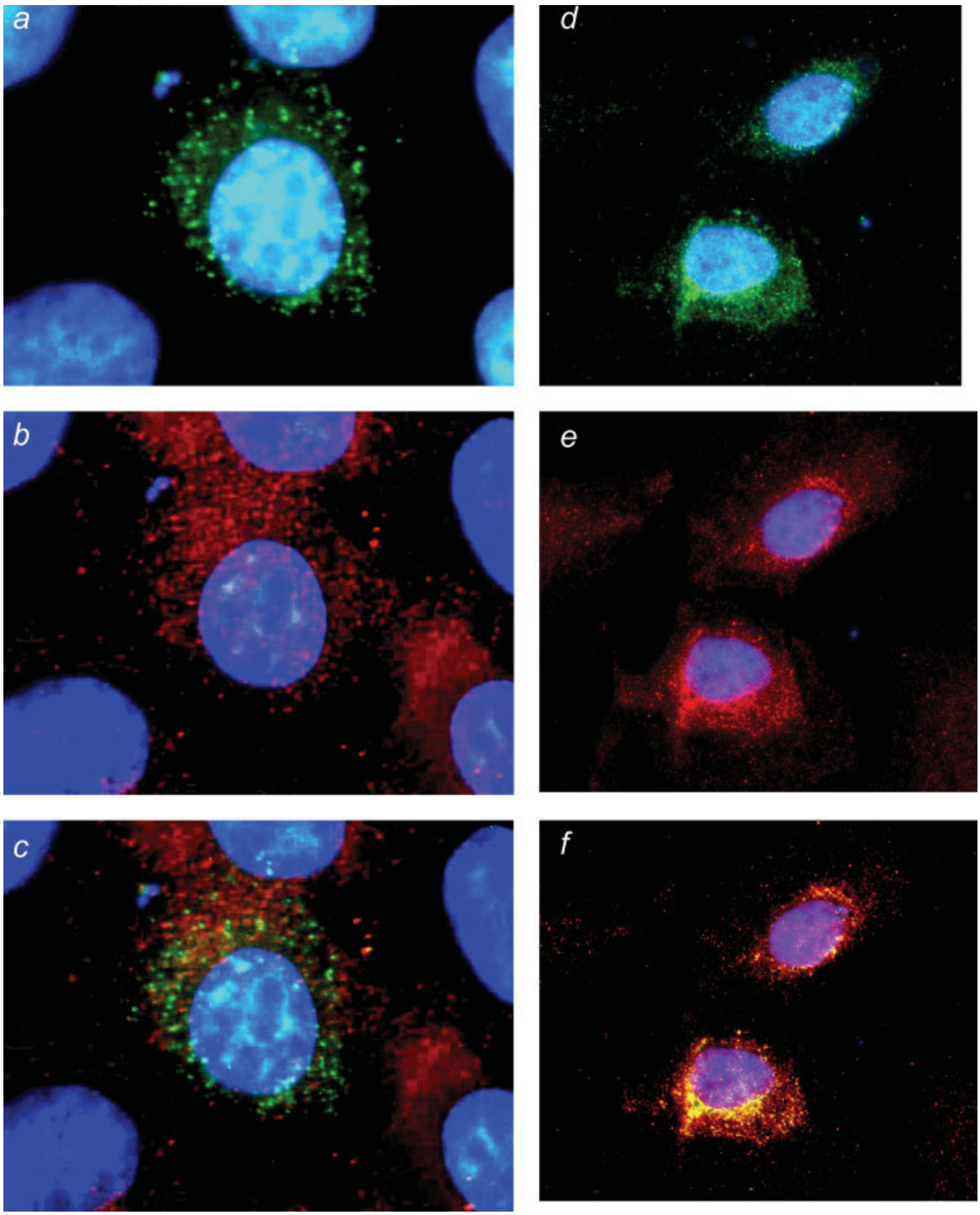

FIGURE 6 – Targeting of GFP-tagged $NRDRB_1$ (*a–c*) and GFP-tagged NRDR (*d–f*) in HeLa cells. Immunofluorescent images of whole cell transfected with $NRDRB_1$-GFP and NRDR-GFP (*a* and *d*, gray spots) and co-stained with peroxisome marker (*b* and *e*, gray spots). The overlay of the 2 images (*a* and *b*) suggests that the 2 signals are predominately not co-localized (*c*) when compared with the peroxisomal localization of NRDR (*f*, gray spots). The nucleus was stained by DAPI. Magnification ×1,000. [Color figure can be viewed in the online issue, which is available at www.interscience.wiley.com.]

graphic films using the ECL kit (Pierce), using the method provided by the supplier. The gels were stained by Coomassie Brilliant Blue to confirm the size of targeted protein.

Immunohistochemistry

Immunohistochemistry was performed on formalin-fixed, paraffin-embedded, human normal cervical epithelium and cervical squamous carcinoma tissues blocks cut at 5-μm thick sections. The serial sections of normal cervical epithelium and tumor tissues were each stained with NRDR and $NRDRB_1$. Briefly, the sections were deparaffinized in xylene, rehydrated through graded ethanol, immersed in 0.1 M citrate buffer (pH 6.0) and then heated at 95°C in a microwave oven for 10 min, to enhance antigen retrieval. The sections were then treated with 2% H_2O_2 for 10 min

at room temperature to inactivate endogenous peroxidase activity. After a blocking step with 10% normal goat serum, the serial sections of normal cervical epithelium and tumor tissues were each stained with $NRDRB_1$ and NRDR antibody diluted to 1:150 and 1:200, respectively, in 3% BSA/PBS overnight at 4°C. Nonimmune antibody instead of the primary antibodies served as a negative control. Subsequently, sections were incubated with a biotinylated goat anti-rabbit IgG, avidin-biotinylated complex and diaminobenzidine. The sections were counterstained with hematoxylin before dehydration, through graded ethanol solutions and xylene, and then coverslipped.

Statistical analysis

Fisher's exact 2-sided probability test was used. A p value <0.05 was considered statistically significant.

Results

Identification of the novel variant $NRDRB_1$ and detection of its mRNA expression in cervical tumors

To identify novel variants of NRDR, we performed RT-PCR for mRNA from HeLa cells using 2 NRDR specific primers (Fig. 1, NRDRF/NRDRR). In addition to the full-length NRDR (638 bp), we identified a short amplification product (536 bp, Fig. 2*b*: H). Sequence analysis revealed that the short PCR product, which lacked the complete coding region of exon 3, encoded an alternatively spliced 244-residue variant of NRDR (Fig. 3). Based on the NRDR nomenclature, this isoform was designated $NRDRB_1$. Using 3′ and 5′RACE, we obtained the full-length cDNA of $NRDRB_1$ (Genbank accession number DQ325464). The coenzyme-binding region of the $NRDRB_1$ N-terminal, the substrate binding part of the C-terminal and partial SDR functional domain were retained (Fig. 3). The predicted molecular mass of $NRDRB_1$ is ~27 kDa and isoelectric point is 9.32, when compared with ~29 kDa and isoelectric point 7.67 of NRDR, respectively.

In the next step, the normal cervical and cervical tumor tissue samples were analyzed for $NRDRB_1$ and full-length NRDR mRNA transcripts. In the RT-PCR experiments, we used a set of oligonucleotide primers that covered the spliced region, which yielded amplification products of 638 bp for the full-length and 536 bp (Fig. 1, NRDR F/R) or 355 bp (Fig. 1, NRDRB1F/NRDRR) for the spliced mRNA (Figs. 2*b* and 2*c*). The results of DNA sequencing of $NRDRB_1$ are shown in Figure 2*a*. PCR products were visualized by ethidium bromide staining. The expected size of PCR amplification products for $NRDRB_1$ transcripts were detected in 14 of 26 (53.9%) cervical tumor tissues, but not in any of the 12 normal cervical tissue samples ($p < 0.05$, compared with cervical tumor tissues). The expression of full-length NRDR was detected in both normal and neoplastic cervical tissue samples (Fig. 2*b*).

To confirm the expression of $NRDRB_1$ and NRDR mRNAs, we carried out the SYBR Green I real-time PCR assay. No amplification of $NRDRB_1$ was detected in normal cervical epithelium (C_t = 40). The expression of $NRDRB_1$ mRNA was detected in 14 of 26 cervical tumor tissues while NRDR mRNA was detected in both the normal and neoplastic cervical epithelia, consistent with the results of RT-PCR. Owing to the difference in product size, $NRDRB_1$ (95 bp) and NRDR (150 bp) could be identified based on their distinctive melting temperatures. No other product was detected, either by analysis of melting temperature curves or after migration of the PCR products on agarose gel. These results indicate that there was no interference or artifact in the reading of the fluorescence, confirming the specificity of the signal.

In addition to $NRDRB_1$, we also detected 2 other splicing variants in neoplastic cervical epithelium; $NRDRB_2$ (Genbank accession number DQ338571, with the deletion of exons 3 and 6) and $NRDRA_1$ (also detected in neuroblastoma, Genbank accession number AY943857, with the deletion of exons 3,4,5 and 6). Both variants were detected in cervical squamous carcinoma tissue samples that were negative for $NRDRB_1$ transcript. However, the proportion of tissue samples positive for the above 2 variants was low (3 cases of $NRDRB_2$ and 2 cases of $NRDRA_1$). Figure 4 provides a schematic comparison of the structures of the 3 variants of NRDR gene in neoplastic cervical tissue samples.

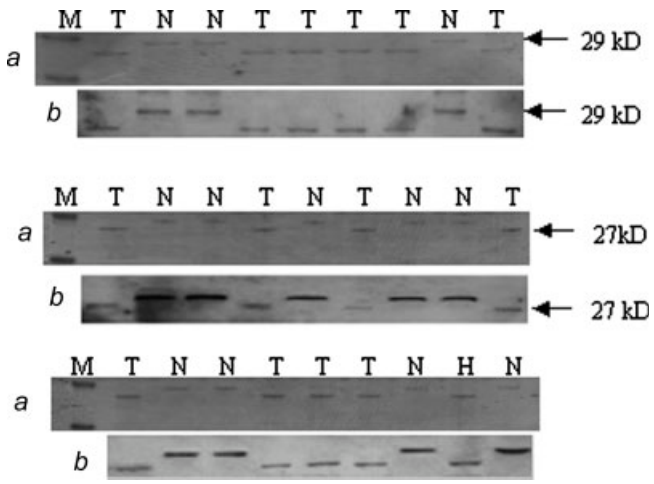

Figure 7 – SDS-PAGE and Western-blot analysis of NRDR and $NRDRB_1$ expression after IP. (*a*) Normal cervix epithelium and cervix squamous carcinoma samples after IP were analyzed by SDS-PAGE and stained by Coomassie R-250. (*b*) Western-blot analysis of NRDR (29 kDa) and $NRDRB_1$ (27 kDa) expression in normal and neoplastic cervix epithelium samples. M: Molecular weight markers. N: normal cervix epithelium samples. T: cervical squamous carcinoma tissues. H: HeLa cell. The normal human cervical tissues showed expression of NRDR, whereas $NRDRB_1$ expressed predominately in cervical tumor tissues confirmed by MALDI-TOF mass spectrometric analysis respectively.

Expression of the recombinant $NRDRB_1$ constructs in E. coli *and production of polyclonal antibody*

The native $NRDRB_1$ protein was obtained using pDEST14 vector of Gateway Expression system. The induced protein comprised 30–50% of the total protein of *E. coli*, and the optimal time for induction was 3 hr. The soluble native protein of $NRDRB_1$ was purified from lysates of *E. coli* BL21-AI, using affinity chromatography (Fig. 5). Hyperimmune rabbit antisera against $NRDRB_1$ were purified using the protein G column on ATKAexplore system, and only highly sensitive polyclonal antibody was used. The specificity assay indicated that the purified antibody could interact with both $NRDRB_1$ protein and NRDR protein, and was thus employed in IP and immunoblot experiments for detection of $NRDRB_1$ and NRDR proteins.

Differences in subcellular localizations of NRDR and $NRDRB_1$

$NRDRB_1$ is a member of the SDR family, and its sequence is composed of a C-terminal SRL tripeptide, which is a variant of Type 1 peroxisomal targeting signal, SKL. To investigate the subcellular localization of $NRDRB_1$, the sequence encoding the GFP was fused in-frame to the amino-terminal of $NRDRB_1$, and the resultant plasmids were transiently transfected into HeLa cells to determine its localization. The merged images showed that NRDR protein, but not $NRDRB_1$ protein, was localized in the peroxisome (Fig. 6).

Expression of $NRDRB_1$ protein in tumor tissue

We next analyzed the expression of the $NRDRB_1$ protein. Because of the low expression levels of $NRDRB_1$ in HeLa cells and cervical tumor tissues, the levels were concentrated by IP using Dynal beads-conjugated rabbit polyclonal antibody of $NRDRB_1$ purified by protein G. The IP proteins were separated by

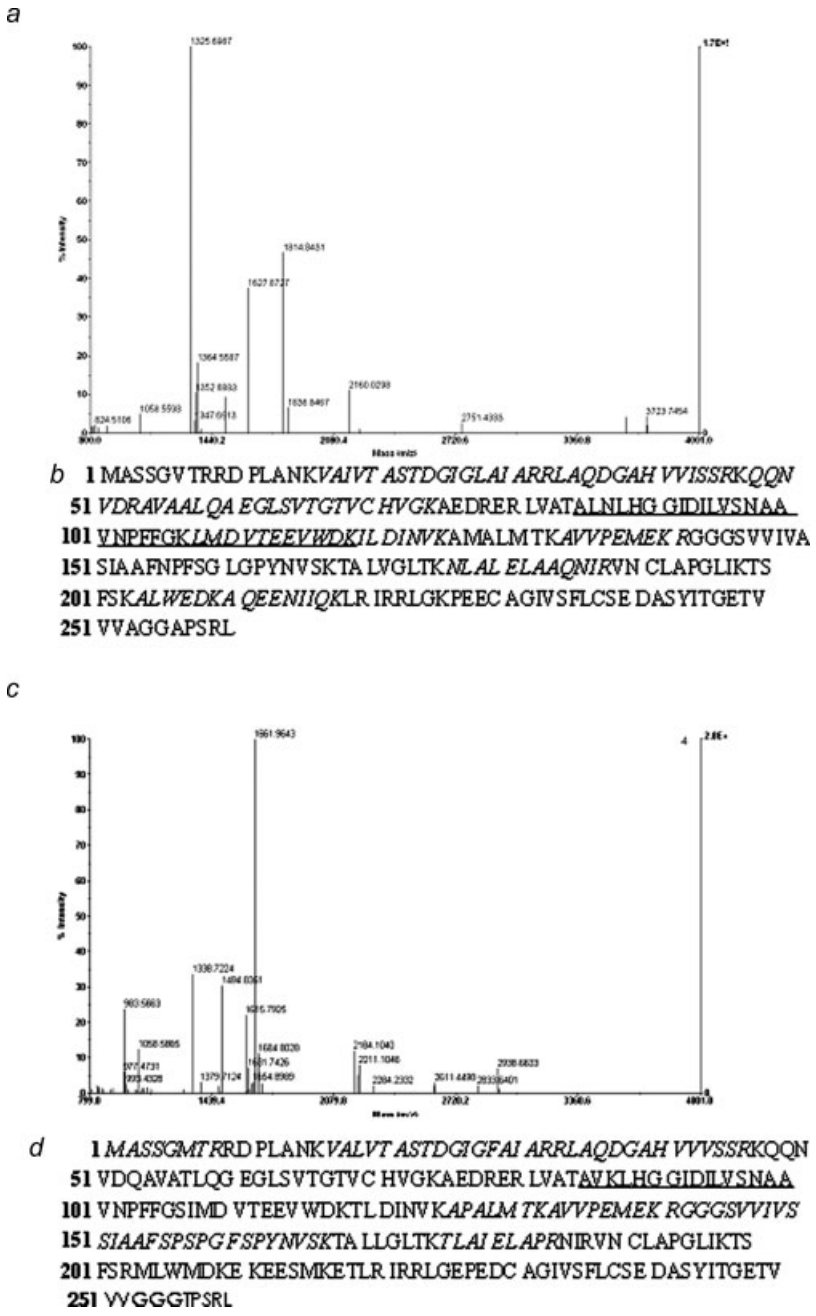

FIGURE 8 – MALDI-TOF mass spectrometric analysis of NRDR and $NRDRB_1$. (*a*) Results of MALDI-TOF mass spectrometric analysis of NRDR. (*b*) Amino acid sequences analyzed for NRDR by PMF analysis and matched peptides shown in bold italic in the full-length sequence of the protein. (*c*) Results of MALDI-TOF mass spectrometric analysis of $NRDRB_1$. (*d*) Amino acid sequences analyzed for $NRDRB_1$ by PMF analysis and matched peptides shown in bold italic in the full-length sequence of the protein. Underlined sequences (in *b* and *d*) showed the region encoded by exon 3.

SDS-PAGE and analyzed by Western blotting (Fig. 7*b*). In the IP proteins, the bands corresponding to NRDR and $NRDRB_1$ were stained by Coomassie Brilliant Blue to confirm the size of targeted protein (Fig. 7*a*) and were cut for MALDI-TOF PMF analysis. The proteins were identified by the PMF method, using Mascot Search on the web (http://www.matrixscience.com/home.html). The results (Fig. 8) showed that full-length NRDR protein was predominately expressed in normal cervical tissues, whereas $NRDRB_1$ protein was detected in HeLa cells and cervical tumor tissues that were also positive for $NRDRB_1$ mRNA. However, in other cervical tumor tissues positive only for NRDR mRNA, we could not detect NRDR protein or $NRDRB_1$ protein.

To determine the cellular distribution of $NRDRB_1$ and NRDR protein expression in normal and neoplastic cervical epithelia, we carried out immunohistochemical staining of the proteins. Figure 9 shows representative staining results of $NRDRB_1$ and NRDR in serial sections. Epithelial basal cells were positive for NRDR in normal cervical epithelium (Figs. 9*a* and 9*b*). In cervical tumor tissues, $NRDRB_1$ protein was abundantly present in tumor cells, although not all cells were positive (Figs. 9*c* and 9*d*). In other cervical tumor tissues positive only for NRDR mRNA, neither NRDR nor $NRDRB_1$ was detected (Figs. 9*e* and 9*f*).

Discussion

In the present study, we identified a new splicing variant of the *NRDR* (*DHRS4*) gene in human cervical squamous carcinoma. The variant, $NRDRB_1$, which lacks the complete coding region of exon 3, was exclusively detected in cervical tumor samples (53.9%, 14/26 cases), but not in the corresponding normal tissues. $NRDRB_1$ protein was also detected in cervical tumors positive for $NRDRB_1$ mRNA. Although many recent studies have identified cancer-specific or cancer-associated splice variants at transcriptional level, the expression of the corresponding protein of the detected splice var-

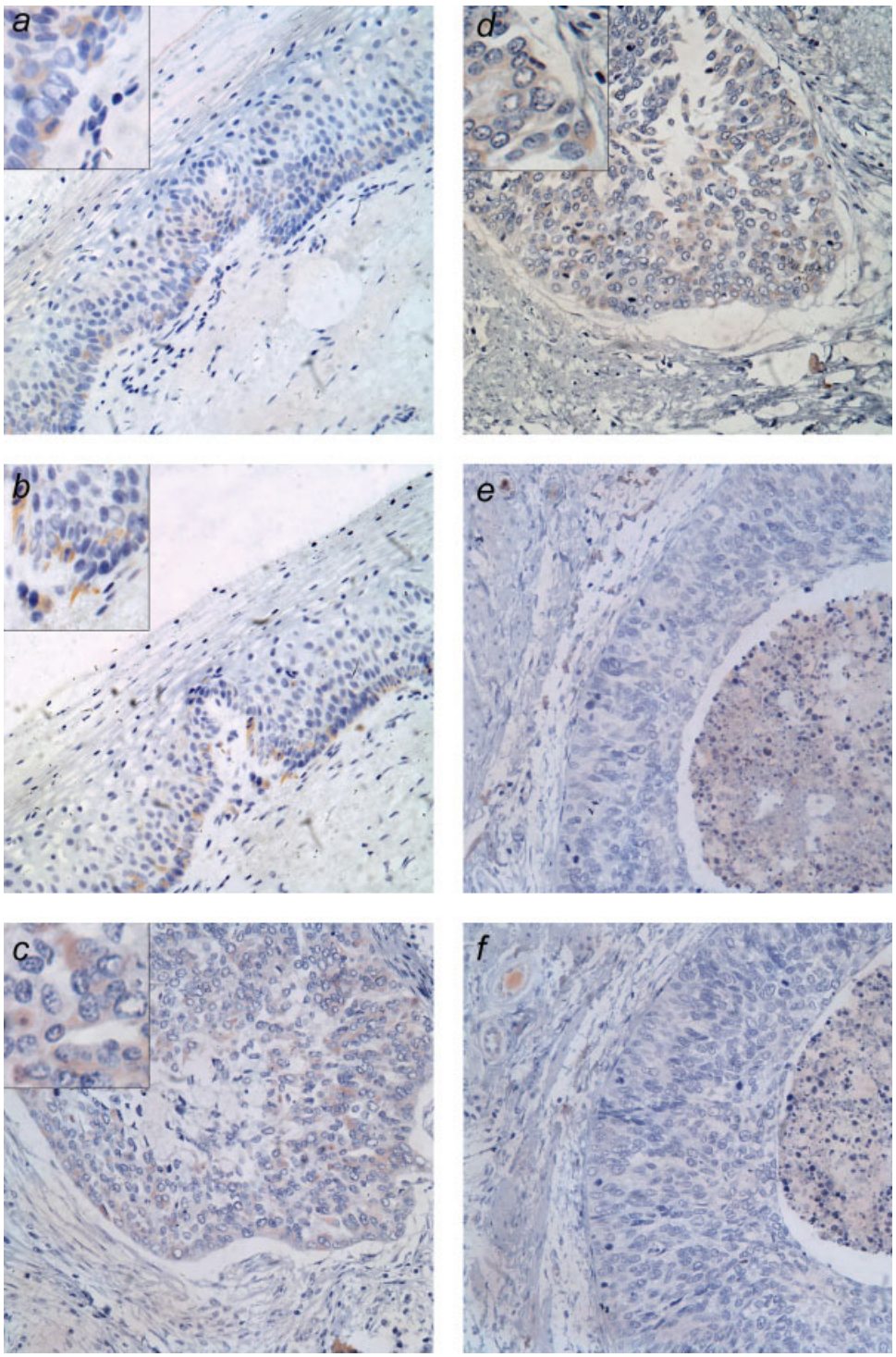

FIGURE 9 – Immunohistochemical staining of $NRDRB_1$ and NRDR proteins in normal cervical epithelium and cervical squamous carcinoma tissues. According to the results of IP and MALDI-TOF peptide mass fingerprint analysis, the serial sections in normal cervical tissues (*a*,*b*) show the expression of NRDR protein. In cervical tumor tissues expressing $NRDRB_1$ mRNA (*c*,*d*), the signals indicate the expression of $NRDRB_1$ protein. In other cervical tumor tissues only expressing NRDR mRNA, neither NRDR nor $NRDRB_1$ was detected (*e*,*f*). (*a*,*c*,*e*) Immunostained with NRDR antibody. (*b*,*d*,*f*) Immunostained with $NRDRB_1$antibody. Magnifications: ×400 (*a–f*); ×800 (insets in *a–d*). [Color figure can be viewed in the online issue, which is available at www.interscience.wiley.com.]

iants was often not verified.[27,29] The results of the present study indicated that the mRNA levels do not directly correlate with the expression levels of functional proteins. In addition, we also identified 2 other splice variants, $NRDRB_2$ and $NRDRA_1$ (Fig. 4). Both of these variants were detected in cervical squamous carcinoma tissue samples negative for $NRDRB_1$ mRNA, but the proportions of tissues positive for $NRDRB_2$ and $NRDRA_1$ variants were low. These findings indicate that abnormal splicing of NRDR exists in cervical tumors, suggesting the possible involvement of these variants in cervical carcinogenesis.

We showed previously that full-length NRDR was localized in the peroxisomes.[5] In present study, we investigated the subcellular localization of $NRDRB_1$, in addition to the localization of full-length NRDR. The immunofluorescence images indicated that $NRDRB_1$ was not localized in peroxisomes, in spite of its C-terminal peroxisomal targeting signal. We noticed that the prototypical SDR residues "LVSNAA" fold[4] was defected in $NRDRB_1$ (Fig. 3), because of alternative splicing. This might impact the folding of $NRDRB_1$ protein, resulting in conformational change, which could alter its subcellular localization and function.

Cervical cancer is the second most common malignancy in women worldwide and a significant health problem.[34] Prevention of cervical cancer and its precursors are therefore important objectives.[34,35] Human papilloma virus (HPV) infection is a major factor in the pathogenesis of cervical cancer.[36,37] Recent studies confirm that retinoids inhibit the proliferation and differentiation of cervical cells infected with HPV, and regulate E6/E7 transcript levels in some cervical cell lines.[38–40] These studies suggest that retinoids may reduce the extent of viral oncogene transcription, and are thus potentially useful in slowing the neoplastic process. The results presented here provide evidence for the possible involvement of metabolic disturbances of RA, based on abnormal splicing and functional disorder of NRDR, in tumorigenesis of cervical carcinoma.

Carcinogenesis consists of multiple steps, and cancer development is associated with accumulation of several genetic and epigenetic events, arising over a long time interval. Inactivation or functional disorders of the splicing mechanism might be an important step in carcinogenesis and cancer development. In some cases, alternative splicing yields protein variants with markedly different and sometimes antagonistic properties.[41–43] Preliminary studies from our laboratories suggest that the enzymatic activity of $NRDRB_1$ is remarkably lower than that of NRDR, with retinol and retinal as substrates. Other activities or functions of $NRDRB_1$ await discovery.

To elucidate the mechanism of production of alternatively spliced variant $NRDRB_1$, we analyzed the sequence of genomic regions in normal and neoplastic cervical tissues. No genomic mutation of the splice site and other splicing-related sequence was detected (data not shown). Although a considerable effort has been made to understand the molecular basis of alternative splicing, the mechanisms leading to splicing defects in cancer are still poorly understood. It has been shown in individual cases that inherited or somatic mutations in cis-regulatory elements, as well as oncogenic signaling and variations in the composition, concentration, localization and activity of trans-acting regulatory factors, may result in changes in splice-site recognition and usage.[21,44] Furthermore, many studies over the last 20 years have reported cancer-specific alternative splicing in the absence of genomic mutations.[45]

Under normal circumstances, the intracellular levels of RA in tissues are tightly controlled. The molecular mechanisms appear to function at several levels of RA metabolism: biosynthesis, degradation and storage. Aberrations in retinoid signaling are early events in carcinogenesis, and vitamin A deficiency is reported to be associated with a higher incidence of cancer.[46] Dietary supplementation of vitamin A and β-carotene appears to decrease the risk of developing cervix cancer.[47] Retinol and other retinoids maintain normal cervical cell function and inhibit the growth of cervical tumors.[16–18]

From a metabolic viewpoint, retinal in epithelium tissue may be either oxidized to bioactive RA by cytosolic ALDHs or it may be reduced to retinol, which can then be esterified for storage.[48] Hence, retinal is positioned at the crossroads of 2 opposite metabolic processes: activation and inactivation of retinoids. The fate of the cellular retinal would depend on the activities and expression levels of local ALDHs and retinal reductases (such as NRDR) that compete for the same retinal substrate. Therefore, changes in the expression level and activity of NRDR could perturb retinoid homeostasis and alter the intracellular RA concentration, leading to abnormal differentiation and high susceptibility to HPV in the cervical epithelium.

To the best of our knowledge, our study is the first to describe a high frequency of $NRDRB_1$ mRNA and protein splice variant in human cervical tumors. Further studies of a larger sample size are required to confirm these results. Although it is possible that progression of human cervical cancer leads to disturbances of the splicing machinery to produce alternatively spliced variants in a tumor-specific manner, the tumor-specific variant $NRDRB_1$ could be useful as a marker for cervical tumor. Further studies, including functional analysis and subcellular localization, are required to uncover the role of this variant in tumorigenesis of the cervical epithelium.

Acknowledgements

We are grateful to Ms. Esther L. Schachter-Tokarz and Mr. Cui Qing-Ping (Department of Oncology, Montefiore Medical Center, Albert Einstein Cancer Center, NY) for helpful suggestions.

References

1. Huang DY, Ichikawa Y. Purification and characterization of a novel cytosolic NADP (H)-dependent retinol oxidoreductase from rabbit liver. Biochem Biophys Acta 1997;1338:47–59.
2. Usami N, Ishikura S, Abe H, Nagano M, Uebuchi M, Kuniyasu A, Otagiri M, Nakayama H, Imamura Y, Hara A. Cloning, expression and tissue distribution of a tetrameric form of pig carbonyl reductase. Chem Biol Interact 2003;143–144:353–61.
3. Du J, Huang DY, Liu GF, Wang GL, Xu XL, Wang B, Zhu L. cDNA cloning of a short isoform of human liver NADP (H)-dependent retinol dehydrogenase/reductase and analysis of its characteristics. Acta Genetica Sinica 2004;31:661–7.
4. Lei Z, Chen W, Zhang M, Napoli JL. Reduction of all-trans-retinal in the mouse liver peroxisome fraction by the short-chain dehydrogenase/reductase RRD: induction by the PPAR α ligand clofibrate. Biochemistry 2003;42:4190–6.
5. Liu GF, Huang DY, Du J, Cui ZS, Song JD. Functional expression of NADP (H)-dependent retinol dehydrogenase/reductase and determination of its subcellular localization. Chin J Cell Biol 2004;26:433–8.
6. Napoli JL. Retinoic acid biosynthesis and metabolism. FASEB J 1996; 10:993–1001.
7. Duester G. Families of retinoid dehydrogenases regulating vitamin A function: production of visual pigment and retinoic acid. Eur J Biochem 2000;267:4315–24.
8. Ulven SM, Gundersen TE, Weedon MS, Landaas VO, Sakhi AK, Fromm SH, Geronimo BA, Moskaug JO, Blomhoff R. Identification of endogenous retinoids, enzymes, binding proteins, and receptors during early postimplantation development in mouse: important role of retinal dehydrogenase type 2 in synthesis of all-transretinoic acid. Dev Biol 2000;220:379–91.
9. Huang DY, Ichikawa Y. Two different enzymes are primarily responsible for retinoic acid synthesis in rabbit liver cytosol. Biochem Biophys Res Commun 1994;205:1278–83.
10. Molotkov A, Fan X, Duester G. Excessive vitamin A toxicity in mice genetically deficient in either alcohol dehydrogenase Adh1 or Adh3. Eur J Biochem 2002;269:2607–12.
11. Freemantle SJ, Spinella MJ, Dmitrovsky E. Retinoids in cancer therapy and chemoprevention: promise meets resistance. Oncogene 2003; 22:7305–15.
12. Okuno M, Kojima S, Matsushima-Nishiwaki R, Tsurumi H, Muto Y, Friedman SL, Moriwaki H. Retinoids in cancer chemoprevention. Curr Cancer Drug Targets 2004;4:285–98.
13. Um SJ, Han HS, Kwon YJ, Park SH, Rho YS, Sin HS, Park JS. Novel retinoic acid derivative ABPN has potent inhibitory activity on cell growth and apoptosis in cancer cells. Int J Cancer 2003;107:1038–46.
14. Drisko JA, Chapman J, Hunter VJ. The use of antioxidant therapies during chemotherapy. Gynecol Oncol 2003;88:434–9.
15. Wendy JH, Lihua L, Roberto JB, Karen KH, Norman MG. Retinoic acid slows progression and promotes apoptosis of spontaneous prostate cancer. Prostate 2004;61:142–52.
16. Romney SL, Palan PR, Duttagupta C, Wassertheil-Smolter S, Wylie J, Miller G, Slagle NS, Lucido D. Retinoids and prevention of cervical dysplasia. Am J Obstet Gynecol 1981;141:890–4.
17. Rafael MY, Wen LZ, Yuvarani SK, Brent R, Yongkui J, David EO. Retinol conversion to retinoic acid is impaired in breast cancer cell lines relative to normal cells. J Cell Physiol 2000;185:302–9.
18. Ngan HY, Collins RJ, Wong KY, Cheung A, Lai CF, Liu YT. Cervical human papilloma virus infection of women attending social hygiene clinics in Hong Kong. Int J Gynecol Obstet 1993;41:75–9.

19. Francois M, Pilar G, Pierre D, Isabelle B, Pastelle K, Sandrine B, Carla E, Serge H. Antioxidant vitamin and mineral supplementation and prostate cancer prevention in the SU.VI.MAX trail. Int J Cancer 2005;116:182–6.
20. Li YF, Liu GF, Song XH, Du K, Huang DY. cDNA cloning of a short isoform of human neuroblastoma NADP (H)-dependent retinol dehydrogenase/reductase and analysis of its characteristics. Teratog Carcinog Mutagen 2005;17:321–6.
21. Faustino NA, Cooper TA. Pre-mRNA splicing and human disease. Genes Dev 2003;17:419–37.
22. Garcia-Blanco MA, Baraniak AP, Lasda EL. Alternative splicing in disease and therapy. Nat Biotechnol 2004;22:535–46.
23. Black DL. Mechanisms of alternative pre-messenger RNA splicing. Annu Rev Biochem 2003;72:291–336.
24. Maniatis T, Tasic B. Alternative pre-mRNA splicing and proteome expansion in metazoans. Nature 2002;418:236–43.
25. Grabowski PJ, Black DL. Alternative RNA splicing in the nervous system. Prog Neurobiol 2001;65:289–308.
26. Venables JP. Alternative splicing in the testes. Curr Opin Genet Dev 2002;12:615–9.
27. Brett D, Hanke J, Lehmann G, Haase S, Delbruck S, Krueger S, Reich J, Bork P. EST comparison indicates 38% of human mRNAs contain possible alternative splice forms. FEBS Lett 2000;474:83–6.
28. Xu Q, Lee C. Discovery of novel splice forms and functional analysis of cancer-specific alternative splicing in human expressed sequences. Nucleic Acids Res 2003;31:5635–43.
29. Wang Z, Lo HS, Yang H, Gere S, Hu Y, Buetow KH, Lee MP. Computational analysis and experimental validation of tumorassociated alternative RNA splicing in human cancer. Cancer Res 2003;63:655–57.
30. Recio JA, Merlino G. Hepatocyte growth factor/scatter factor induces feedback up-regulation of CD44v6 in melanoma cells through Egr-1. Cancer Res 2003;63:1576–82.
31. Line A, Slucka Z, Stengrevics A, Li G, Rees RC. Altered splicing pattern of TACC1 mRNA in gastric cancer. Cancer Genet Cytogenet 2002;139:78–83.
32. Matsumoto R, Tada M, Nozaki M, Zhang CL, Sawamura Y, Abe H. Short alternative splice transcripts of the mdm2 oncogene correlate to malignancy in human astrocytic neoplasm. Cancer Res 1998;58: 609–13.
33. Asai DJ. Methods in cell biology, vol. 37. San Diego: Academic Press, 1993. 19–50.
34. Parkin DM, Pisani P, Folay J. Estimates of the worldwide incidence of 18 major cancers in 1985. Int J Cancer 1993;54:594–606.
35. Monsonego J, Bosch FX, Coursaget P, Cox JT, Franco E, Frazer I, Sankaranarayanan R, Schiller J, Singer A, Wright TC, Jr, Kinney W, Meijer CJ, et al. Cervical cancer control, priorities and new directions. Int J Cancer 2004;108:329–33.
36. Walboomers JM, Jacobs MV, Manos MM, Bosch FX, Kummer JA, Shah KV, Snijders PJ, Peto J, Meijer CJ, Munoz N. Human papillomavirus is a necessary cause of invasive cervical cancer worldwide. J Pathol 1999;189:12–19.
37. Beskow AH, Engelmark MT, Magnusson JJ, Gyllensten UB. Interaction of host and viral risk factors for development of cervical carcinoma in situ. Int J Cancer 2005;117:690–2.
38. Choo CK, Rorke EA, Eckert RL. Retinoid regulation of cell differentiation in a series of human papillomavirus type 16-immortalized human cervical epithelial cell lines. Carcinogenesis 1995;16:375–81.
39. Agarwal C, Rorke EA, Irwin JC, Eckert RL. Immortalization by human papillomavirus type 16 alters retinoid regulation of human ectocervical epithelial cell differentiation. Cancer Res 1991;51:3982–9.
40. Gasowska-Giszczak U, Darmochwal-Kolarz D, Kwasniewska A, Dziubinska-Parol I, Rolinski J, Oleszczuk J. Apoptosis of HeLa cell lines incubated with retinol. Eur J Obstet Gynecol Reprod Biol 2005; 119:119–22.
41. Okada S, Kao AW, Ceresa BP, Blaikie P, Margolis B, Pessin JE. The 66-kDa Shc isoform is a negative regulator of the epidermal growth factor-stimulated mitogen-activated protein kinase pathway. J Biol Chem 1997;272:28042–9.
42. Srinivasula SM, Ahmas M, Guo Y, Zhan Y, Lazebnik Y, Fernandes-Alnemri T, Alnemri ES. Identification of an endogenous dominant-negative short isoform of caspase-9 that can regulate apoptosis. Cancer Res 1999;59:999–1002.
43. Garneau D, Revil T, Fisette JF, Chabot B. Heterogeneous nuclear ribonucleoprotein F/H proteins modulate the alternative splicing of the apoptotic mediator Bcl-x. J Biol Chem 2005;280:22641–50.
44. Kalnina Z, Zayakin P, Silina K, Line A. Alterations of pre-mRNA splicing in cancer. Genes Chromosomes Cancer 2005;42:342–57.
45. Venables JP. Aberrant and alternative splicing in cancer. Cancer Res 2004;64:7647–54.
46. Sun SY, Lotan R. Retinoids and their receptors in cancer development and chemoprevention. Crit Rev Oncol Hematol 2002;41:41–55.
47. Reina GC, Xavier CE, Xavier B, Carlos AG. The role of diet and nutrition in cervical carcinogenesis: a review of recent evidence. Int J Cancer 2005;117:629–37.
48. Sporn MB, Roberts AB, Goodman DS, eds. The retinoids: biology, chemistry and medicine. New York: Raven, 1994. 229–50.